Computers and Concrete, *Vol. 22, No. 1 (2018) 11-25*
DOI: https://doi.org/10.12989/cac.2018.22.1.011

Flexural analysis of steel fibre-reinforced concrete members

Constantin E. Chalioris* and Thomas A. Panagiotopoulos[a]

Department of Civil Engineering, Scholl of Engineering, Democritus University of Thrace, Laboratory of Reinforced Concrete and Seismic Design of Structures, Xanthi 67100, Greece

(Received June 12, 2017, Revised March 29, 2018, Accepted April 4, 2018)

Abstract. A numerical approach for the evaluation of the flexural response of Steel Fibrous Concrete (SFC) cross-sections with arbitrary geometry, with or without conventional steel longitudinal reinforcing bars is proposed. Resisting bending moment versus curvature curves are calculated using verified non-linear constitutive stress-strain relationships for the SFC under compression and tension which include post-peak and post-cracking softening parts. A new compressive stress-strain model for SFC is employed that has been derived from test data of 125 stress-strain curves and 257 strength values providing the overall compressive behaviour of various SFC mixtures. The proposed sectional analysis is verified using existing experimental data of 42 SFC beams, and it predicts the flexural capacity and the curvature ductility of SFC members reasonably well. The developed approach also provides rational and more accurate compressive and tensile stress-strain curves along with bending moment versus curvature curves with regards to the predictions of relevant existing models.

Keywords: concrete constitutive models; design codes; reinforced concrete (RC); steel fibre-reinforced concrete; structural analysis/design

1. Introduction

The addition of short discontinuous steel fibres in concrete as mass reinforcement has long been recognized that enhances the inherent limitations of concrete such as the inadequate tensile stress-strain behaviour and the lack of post-cracking ductility. Steel fibre-reinforced concrete or else Steel Fibrous Concrete (SFC) exhibits ameliorated mechanical characteristics and increased fracture energy dissipation capacity. Fibrous concrete members demonstrate increased deformation capabilities and pseudo-ductile behaviour due to the gradual debonding procedure of the individual, randomly oriented steel fibres that bridge the developed cracks (Aslani and Nejadi 2012, Spinella *et al*. 2012, Chalioris 2013a, Fu *et al*. 2014, Aslani *et al*. 2014).

Steel fibres was found to be a promising non-conventional reinforcement in shear-critical beams due to the advantageous cracking performance of SFC which, under specific circumstances, alters the brittle shear failures to ductile flexural ones. Thus, the potential partial or total replacement of common steel stirrups with steel fibres, especially in cases where design criteria recommend high transverse steel ratio that leads to short stirrup spacing has been investigated (Greenough and Nehdi 2008, Chalioris and Sfiri 2011, Spinella *et al*. 2010, Colajanni *et al*. 2012, Spinella 2013, Chalioris 2013b, Cuenca *et al*. 2015, Jain and Singh 2016). The incorporation of steel fibres into shear-critical concrete beam-column joints subjected to reversal loading for the enhancement of the entire structural response has also been addressed and broadened the application of SFC to seismically vulnerable members (Tsonos 2009a, 2009b, Abbas *et al*. 2014, Campione 2015).

The favourable influence of steel fibres on the bending strength and overall flexural behaviour of SFC members with or without conventional longitudinal reinforcement has long been acknowledged. Results of several experimental studies revealed that the flexural resistance, ductility, stiffness and energy absorption capacity of SFC beams is considerably increased with an increase of fibre content (Kotsovos *et al*. 2007, Soulioti *et al*. 2011, Amato *et al*. 2011, Kara and Dundar 2012, Zeris *et al*. 2009, Nehdi *et al*. 2015). Analytical models have also been developed to estimate the flexural strength of concrete beams reinforced with common steel reinforcing bars and steel fibres. Generally, these methods ignore the contribution of the steel fibres in compression and evaluate the supplementary tensile strength of the fibrous concrete as an extra flexural strength component that is added to the strength of the tensional steel bars (Barros and Figueiras 1999, Amato *et al*. 2011, Chalioris 2013a, Abbas *et al*. 2014, Singh 2015, 2016). Further, the relevant and well-known Code provisions of the Italian Norm (CNR 2007), RILEM reports (RILEM TC 162-TDF, 2003) and TR63 guidelines (TR63 2007) for the design of SFC members under bending moment adopt simple compressive and tensile stress-strain laws in order to simplify computations and to provide hand calculations. Only a few flexural models take into account the ameliorated stress-strain behaviour of SFC under compression (Campione and Mangiavillano 2008, Campione 2015).

In this study a new numerical approach for the evaluation of the flexural capacity and the ductile response of SFC cross-sections is proposed. Equations with feasible

*Corresponding author, Associate Professor
E-mail: chaliori@civil.duth.gr
[a]Ph.D. Student

ISSN: 1598-8198 (Print), 1598-818X (Online)

software implementation are derived. The developed model calculates the resisting bending moment versus curvature curve of a SFC structural member with arbitrary cross-sectional geometry, with or without conventional steel longitudinal reinforcing bars. Sectional analysis under bending moment and axial force is achieved using refined and verified non-linear laws for SFC that include softening response under compression and tension. The adopted constitutive stress-strain relationship for SFC under compression is derived using test results from an experimental program of 27 compressive tests and an existing database. The total database includes 125 stress-strain curves and 257 strength values providing the overall compressive behaviour of SFC mixtures with various concrete strengths, types and volume fractions of steel fibres. Special tri-linear and linear-exponential stress-strain laws with post-cracking softening part for SFC under tension that are based on experimental observations and existing empirical considerations are also employed.

The validity of the proposed model is checked through extensive comparisons between analytical predictions and test data of 42 SFC beam specimens. From these comparisons, it is observed that the developed approach predicts accurately the flexural capacity and ductility, and yields well-fitted bending moment versus curvature analytical curves to the corresponding test data. Further, it provides rational and more accurate results concerning the compressive and the tensile response of SFC mixtures, and the curvature ductility, the resisting bending moment and the curvature at ultimate of SFC cross-sections with regards to the predictions of existing models.

2. Compressive behaviour of steel fibrous concrete

It is known that the compressive behaviour of SFC is influenced by the properties of its constituent materials and especially by the volume fraction, the aspect ratio and the bond characteristics of the steel fibres added (Ashour *et al.* 2000, Wang *et al.* 2010, Marar *et al.* 2011). Although for small amounts of steel fibres the compressive strength is negligibly increased, the post-peak compressive behaviour seems to be improved exhibiting a noticeable post-cracking ductility response. Several models and analytical relationships have been proposed in the literature to simulate the stress-strain behaviour of fibrous concrete under compression (Nataraja *et al.* 1999, Unal *et al.* 2007, Oliveira Júnior *et al.* 2010, Cagatay and Dincer 2011, Pawade *et al.* 2011, Aslani and Natoori 2013). Most of them are based on test data regression analysis in order to estimate a factor that considers the influence of fibres and depends on many parameters. They are usually valid for fibrous concrete mixtures with specific properties (short-ranged of concrete strength and amount or type of fibres) and predict the entire pre-peak and post-peak compressive response.

The compressive model suggested in this study utilizes empirical formulas derived from test results of a broad range of parametrical studies and is applicable to the analysis and design of SFC members. A recent experimental program of 27 compressive tests that enrich the existing database from the literature (125 stress-strain curve and 257 strength values) providing the entire stress-strain behaviour of SFC mixtures with various concrete strengths, types and volume fractions of steel fibres is also included (Chalioris and Liotoglou 2015). Typical test results of this experimental program are presented in Fig. 1 in terms of compressive stress-strain curves for several amounts of fibres. Cylinders with dimensions of diameter/height = 150/300 mm were cast from the plain concrete batches to be used as reference specimens and from the batches of each SFC mixture. The specimens were tested 28 days after casting under uniaxial compression using a universal testing machine with a maximum capacity of 3000 kN and under displacement control mode at a constant rate of stain (about 2 mm per min). Before performing the test, a layer of special cement was applied on the top and bottom surface of the specimens, to ensure the flatness of their surface. Axial platen-to-platen deformations of the cylinders were recorded with the measurement of linear electronic strain gauges. In order to avoid the disturbance of the extensometer's gauge reading by the cracks formed on the concrete surface, “O” rings at the middle third of the specimen were also used. Lateral deformations have not been measured. The measurements of the applied load and the corresponding axial displacement converted to the compressive stress and strains shown in Fig. 1.

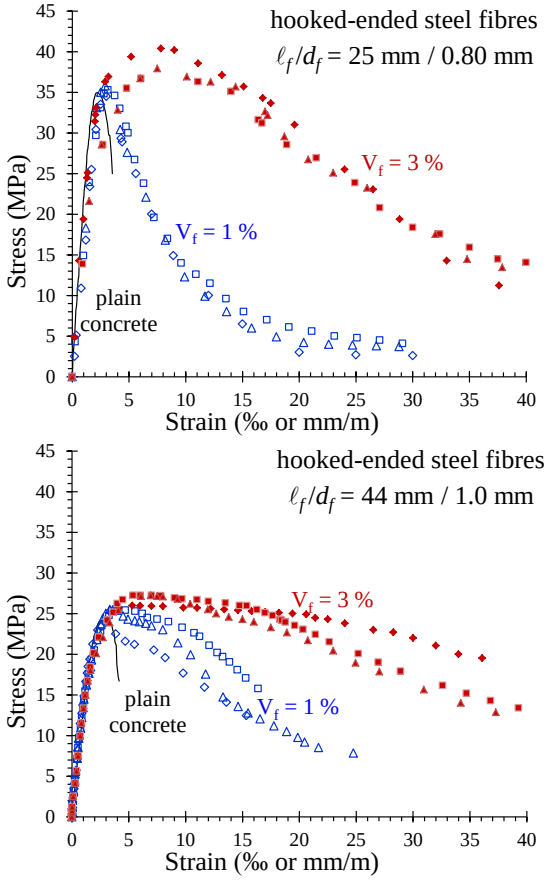

Fig. 1 Experimental data of plain and steel fibrous concrete under compression

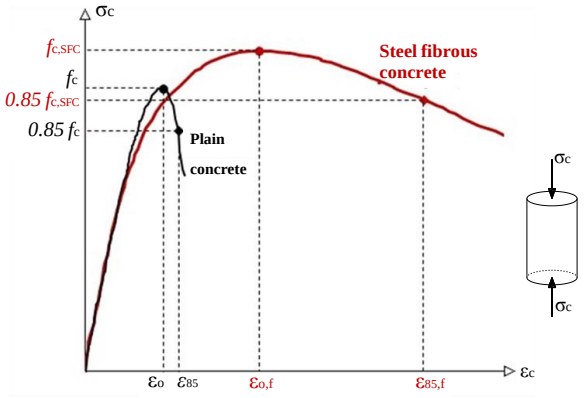

(a)

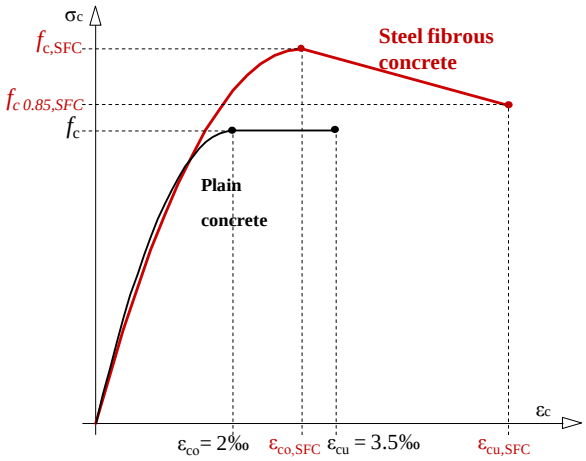

(b)

Fig. 2 (a) Typical and (b) simplified stress-strain curves for SFC and plain concrete under compression

These experimental results reveal that the addition of steel fibres in the concrete marginally increases the compressive strength and, mainly, increases the strain at peak stress and the ultimate strain at failure. The post-peak softening part of the SFC curves in Fig. 1 clearly demonstrates a significant improvement with regards to the plain concrete brittle behaviour. This is attributed to the fact that after the first cracking of concrete the added steel fibres provide increased confinement characteristics and crack-bridging of the formed cracks by the developing of transverse tensional stresses and resist to the crack growth. This favourable characteristic has also been acknowledged and studied in SFC beams under torsion (Chalioris and Karayannis 2009).

The progressive debonding failure of a number of fibres through the developed cracks gives to the fibrous concrete a pseudo-ductile character under compression, and ultimately SFC exhibits improved performance, increased ductility and enhanced mechanical properties compared to the plain concrete (Manolis *et al*. 1997, Soulioti *et al*. 2011). Typical experimental and simplified compressive stress-strain curves of plain and steel fibrous concrete are presented and compared in Fig. 2 (Chalioris and Liotoglou 2015). For comparison reasons the idealized compressive stress-strain relationship given by EC2 (CEN 2004) has been adopted for the case of plain concrete.

The numerical simulation of the SFC response under compression is achieved using simplified analytical relationships and is divided into two parts, as shown in Fig. 2. The first part describes the ascending stress-strain behaviour to the point of the ultimate stress, while the second one describes the post-peak descending softening part after the maximum compressive strength. The first stage ($\varepsilon_c \leq \varepsilon_{co,SFC}$) is simulated by the well-known Hognestad parabola according to the following expression (CEN 2004)

$$\sigma_c = f_{c,SFC}\left[1-\left(1-\frac{\varepsilon_c}{\varepsilon_{co,SFC}}\right)^n\right] \quad (1)$$

$$n = \begin{cases} 2 & f_{c,SFC} \leq 50 \text{ MPa} \\ 1.4 + 23.4\left[\dfrac{90 - f_{c,SFC}}{100}\right]^4 & f_{c,SFC} > 50 \text{ MPa} \end{cases} \quad (2)$$

where $f_{c,SFC}$=the cylinder compressive strength of SFC, $\varepsilon_{co,SFC}$=the strain that corresponds to the ultimate stress-compressive strength.

Test data from 20 experimental works around the world are also used as database (Tan *et al*. 1993, Ashour and Wafa 1993, Ashour *et al*. 2000, Gao *et al*. 1997, Barros and Figueiras 1999, Nataraja *et al*. 1999, Padmarajaiah and Ramaswamy 2001, Daniel and Loukili 2002, Kwak *et al*. 2002, Song and Hwang 2004, Duzgun *et al*. 2005, Yazici *et al*. 2007, Köksal *et al*. 2008, Unal *et al*. 2007, Mohammadi *et al*. 2008, Oliveira Júnior *et al*. 2010, Marar *et al*. 2011, Pawade *et al*. 2011, Nili and Afroughsabet 2012, Chalioris 2013b) in order to determine the value of the parameters that determine the SFC overall compressive behaviour. These parameters are (i) the strength, $f_{c,SFC}$, (ii) the strain at ultimate strength, $\varepsilon_{co,SFC}$, and (iii) the ductility factor, μ_{85}, that equals to the ratio of the maximum considered strain, $\varepsilon_{cu,SFC}$, to the strain at ultimate strength, $\varepsilon_{co,SFC}$ (Chalioris and Liotoglou 2015).

The values of the aforementioned three parameters as derived from the tests of the database have been related in the diagrams of Fig. 3 with the corresponding test data of the known fibre factor, F, which was first proposed by Narayanan and Darwish (1987)

$$F = \beta V_f \frac{\ell_f}{d_f} \quad (3)$$

where β=the fibre bond factor considering shape and surface characteristics of fibre and can be taken as 0.75 for deformed fibres, 0.50 for round fibres and 1.0 for indented fibres, V_f=the volume fraction of the fibres, ℓ_f=the fibre length, d_f=the fibre diameter.

In the diagrams of Figs. 3(a) and (b) the compressive strength values, $f_{c,SFC}$, are related with the values of the fibre factor, F, derived from 257 test data (147 of normal and 110 of high concrete strength, respectively). The experimental database includes SFC mixtures that contain short steel fibres with aspect ratio ℓ_f/d_f from 20 to 114 and volume fraction $V_f \leq 3\%$. The values of the normal and the high concrete strength range from 10.87 to 49.88 MPa and from 55.58 to 102.40 MPa, respectively. Further, the ultimate increase of the compressive strength due to the addition of

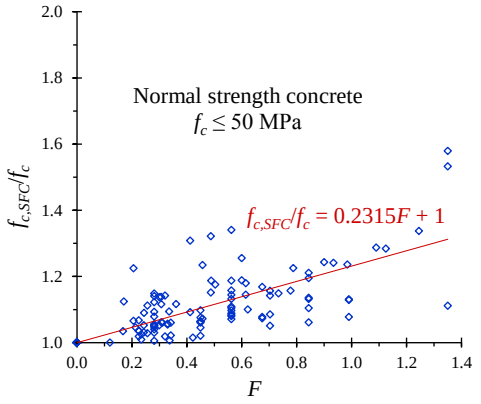

(a)

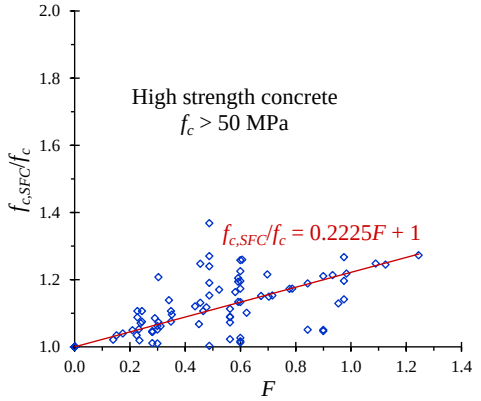

(b)

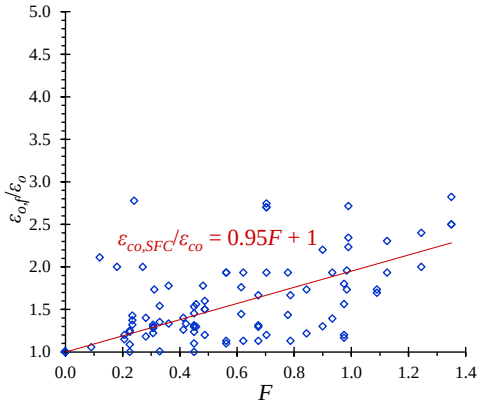

(c)

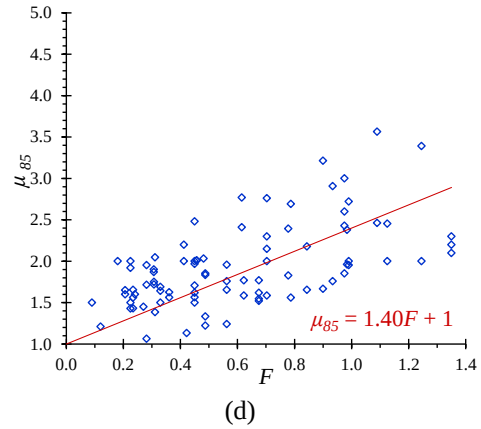

(d)

Fig. 3 Relationship of the fibre factor, F, with the compressive (normal and high) strength, the strain at peak-stress and the ductility parameter

the steel fibres is 36.7% and 26.9% for the examined cases in Figs. 3(a) and (b), respectively.

The following relationship between the increase of the compressive strength due to the addition of the steel fibres ($f_{c,SFC}$ is the SFC strength and f_c is the corresponding plain concrete strength) and the fibre factor, F, for normal strength (≤50 MPa) and high strength concrete (>50 MPa) is obtained from regression analysis (see Figs. 3(a) and (b))

$$f_{c,SFC} = \begin{cases} f_c\left(0.2315F + 1\right) & f_c \le 50 \text{ MPa} \\ f_c\left(0.2225F + 1\right) & f_c > 50 \text{ MPa} \end{cases} \quad (4)$$

Further, the strain values derived from 125 compressive stress-strain curves of the test database are used in Figs. 3(c) and (d) in order to determine the relationship between the compressive strain at ultimate strength of the SFC, $\varepsilon_{co,SFC}$, and the ductility factor, $\mu_{85}=\varepsilon_{cu,SFC}/\varepsilon_{co,SFC}$, with the values of the fibre factor, F, respectively. The experimental database includes SFC mixtures that contain short steel fibres with aspect ratio ℓ_f/d_f from 31 to 114 and volume fraction V_f≤3%. The concrete strength ranges from 18.14 to 93.56 MPa, the SFC compressive strain at ultimate strength ranges from 0.0015 to 0.0132 and the maximum considered strain ranges from 0.0022 to 0.0296.

Thus, the influence of the fibre factor, F, to the increase of the compressive strain at ultimate strength, $\varepsilon_{co,SFC}$, due to the addition of steel fibres with regards to the corresponding plain concrete strain, ε_{co} (usually ε_{co}=2‰) is also obtained from regression analysis (see also Fig. 3(c))

$$\varepsilon_{co,SFC} = \varepsilon_{co}\left(0.95F + 1\right) \quad (5)$$

The post-peak response of SFC is assumed herein linear from the value of the ultimate strength, $f_{c,SFC}$, until the point of stress that equals to: $f_{c0.85,SFC}=0.85f_{c,SFC}$ (see also Fig. 2(b)). This stress-strain point of the 85% of the ultimate strength is assumed as the end of the reliable post-peak response range. Thus, the maximum considered strain of the SFC, $\varepsilon_{cu,SFC}$, that corresponds at this specific point is related to the strain at ultimate strength, $\varepsilon_{co,SFC}$, the ductility factor, μ_{85}, and the fibre factor, F, based on the regression analysis (Fig. 3(d)) and by the expressions

$$\varepsilon_{cu,SFC} = \varepsilon_{co,SFC}\mu_{85} \quad (6)$$

$$\mu_{85} = 1.40F + 1 \quad (7)$$

This way, the following equations can be used to relate the compressive stress to the strain at each stage

$$\sigma_c = \begin{cases} f_{c,SFC}\left[1-\left(1-\dfrac{\varepsilon_c}{\varepsilon_{co,SFC}}\right)^n\right] \\ \text{if } 0 \le \varepsilon_c \le \varepsilon_{co,SFC} \\ \\ f_{c,SFC}\left[1-0.15\dfrac{\varepsilon_c-\varepsilon_{co,SFC}}{\varepsilon_{cu,SFC}-\varepsilon_{co,SFC}}\right] \\ \text{if } \varepsilon_{co,SFC} < \varepsilon_c \le \varepsilon_{cu,SFC} \end{cases} \quad (8)$$

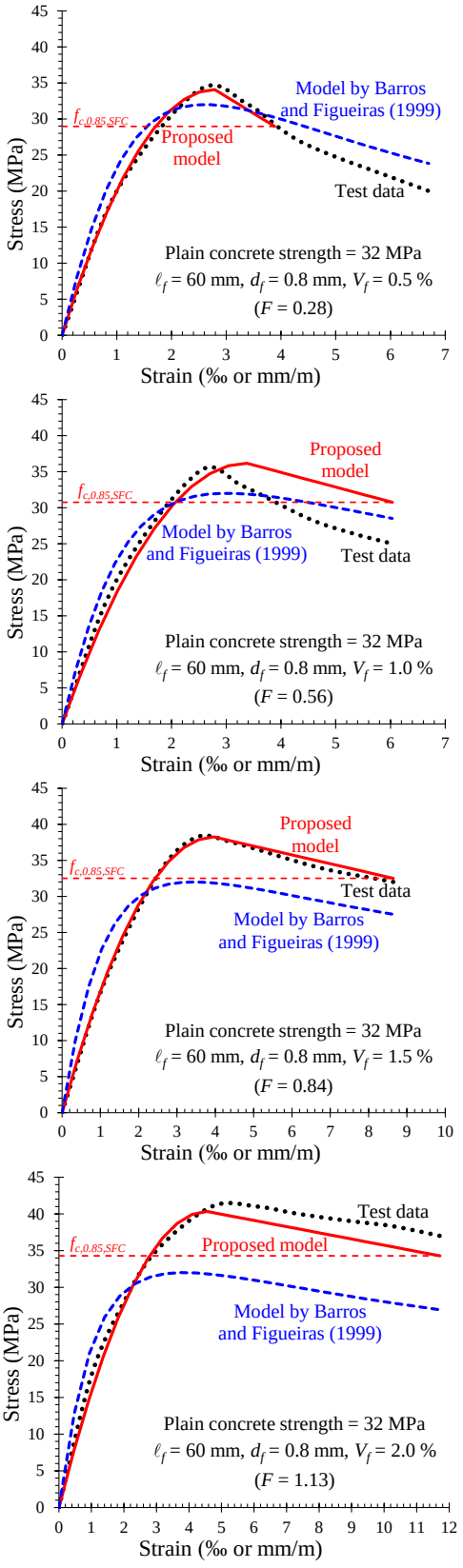

Fig. 4 Comparisons of the compressive stress-strain curves

In order to comprehend the ability and the accuracy of the proposed analytical model to describe the entire compressive stress-strain relationship of SFC with various amounts of short steel fibres, Fig. 4 has been illustrated. In Fig. 4 the experimental compressive behaviour of SFC with four different volume fractions (V_f=0.5%, 1%, 1.5% and 2%) from the uniaxial compression tests of Marar *et al.* (2011) (black dotted lines) are compared with the analytically predicted stress-strain curves derived from the proposed approach (red continuous lines) and the model reported in Barros and Figueiras (1999) (blue dashed lines). It is obvious that the increased compressive strength and the enhanced post-peak response of the SFC with regards to the plain concrete behaviour are important parameters that significantly affect the stress-strain relationship of the SFC under compression and the proposed model curves are in a very good agreement with the experimental ones.

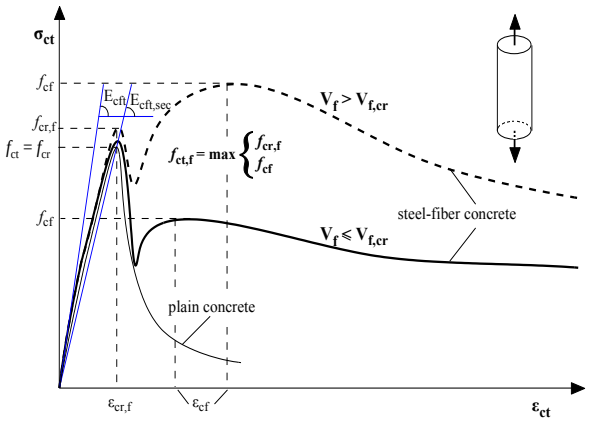

Fig. 5 Typical tensile stress-strain curves

3. Tensile behaviour of steel fibrous concrete

The tensional response of the SFC is mainly linear until the tensile stress reaches the characteristic value termed as cracking stress, $f_{cr,f}$, which is usually equal or slightly higher from the ultimate tensile strength of the plain concrete, f_{ct} or f_{cr}, as shown in the curves of Fig. 5 (Karayannis 2000a). The corresponding strain at this cracking stress is termed as $\varepsilon_{cr,f}$.

The ultimate post-cracking tensile stress, f_{cf}, is either less or greater than the cracking stress, $f_{cr,f}$, depending on the value of the critical volume fraction, $V_{f,cr}$, as shown in Fig. 5 (Naaman 2003). The evaluation of this critical volume fraction is based on the following expressions

$$V_{f,cr} = \frac{f_{ct}}{n_\ell n_o \sigma_{fu}} \tag{9}$$

where n_ℓ=the ratio of the average fibre stress to the maximum fibre stress, n_o=fibre orientation factor in the elastic range, σ_{fu}=the ultimate stress of the fibre when a uniform ultimate bond stress, τ_u, is assumed at the fibre - matrix interface

$$n_o = 0.405 \tag{10}$$

$$n_\ell = \begin{cases} 0.50 & \ell_f \leq \ell_{cr} \\ 1 - \dfrac{\ell_f}{2\ell_{cr}} & \ell_f > \ell_{cr} \end{cases} \tag{11}$$

$$\sigma_{fu}=\begin{Bmatrix} 2\tau_u \dfrac{\ell_f}{d_f} & \ell_f \le \ell_{cr} \\ f_{uf} & \ell_f > \ell_{cr} \end{Bmatrix} \quad (12)$$

where ℓ_{cr}=the length required to develop in the fibre the ultimate fibre stress, ℓ_{fr}=the embedded length of the fibre, P_u=the ultimate pull-out force, f_{uf}=the steel fibre ultimate tensile strength (Karayannis 2000b)

$$\ell_{cr}=0.5\,f_{uf}\frac{d_f}{\tau_u} \quad (13)$$

$$\tau_u=\frac{P_u}{\pi d_f \ell_{fr}} \quad (14)$$

This way, the suggested analytical approach includes two types of tensile stress-strain curves depending on the relation between the actual volume fraction of the added steel fibres, V_f, and the critical one, $V_{f,cr}$. If $V_f \le V_{f,cr}$ then the ultimate post-cracking tensile stress, f_{cf}, is less than the cracking stress, $f_{cr,f}$, and a tri-linear model is used as shown in Fig. 6(a). If $V_f > V_{f,cr}$ then $f_{cf} > f_{cr,f}$ and a linear-exponential model is used as shown in Fig. 6(b).

The elastic first linear part of both models is determined by the values of the cracking strain $\varepsilon_{cr,f}$, and the secant modulus of elasticity, $E_{cft,sec}$, at the cracking stress, $f_{cr,f}$

$$\varepsilon_{cr,f}=n_\ell n_{oe} V_f\left(\varepsilon_{yf}-\varepsilon_{cr}\right)+\varepsilon_{cr} \quad (15)$$

$$E_{cft,\sec}=\frac{3}{8}E_{cfL,\sec}+\frac{5}{8}E_{cfT,\sec} \quad (16)$$

$$f_{cr,f}=\varepsilon_{cr,f}E_{cft,\sec} \quad (17)$$

where n_{oe}=the fibre orientation factor in the elastic range (= 0.167 for concrete mixtures and 0.200 for mortar mixtures according to Bentur and Mindess (2007), ε_{cr}=the cracking strain of the plain concrete that corresponds to the plain concrete ultimate tensile strength, f_{ct} or f_{cr}, ε_{yf}=the yield strain of the steel fibre

$$\varepsilon_{yf}=\frac{f_{uf}}{E_f} \quad (18)$$

$$E_{cfL,\sec}=E_{ct,\sec}\left(1-V_f\right)+E_f V_f \quad (19)$$

$$E_{cfT,\sec}=\frac{E_f E_{ct,\sec}}{E_f(1-V_f)+E_{ct,\sec}V_f} \quad (20)$$

$$E_{ct,\sec}=\frac{f_{ct}}{\varepsilon_{cr}} \quad (21)$$

- Tri-linear model: $V_f \le V_{f,cr}$ and $f_{cf} \le f_{cr,f}$: The ultimate tensile strength of SFC, $f_{ct,f}$, the post-cracking stress, f_{cf}, and the corresponding strain, ε_{cf}, are calculated by the following expressions (Karayannis 1995)

$$f_{ct,f}=f_{cr,f}=\varepsilon_{cr,f}E_{cft,\sec} \quad (22)$$

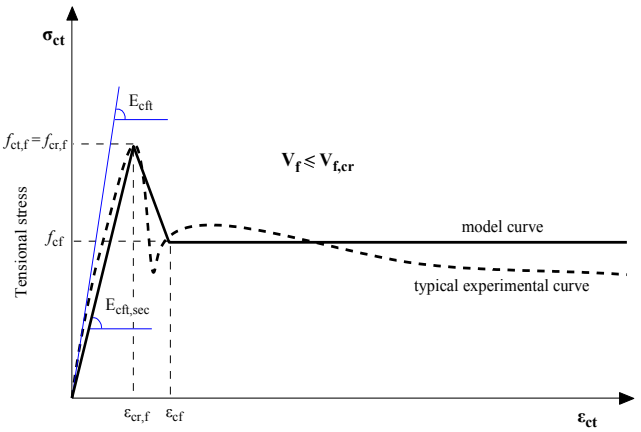

(a) Tri-linear model

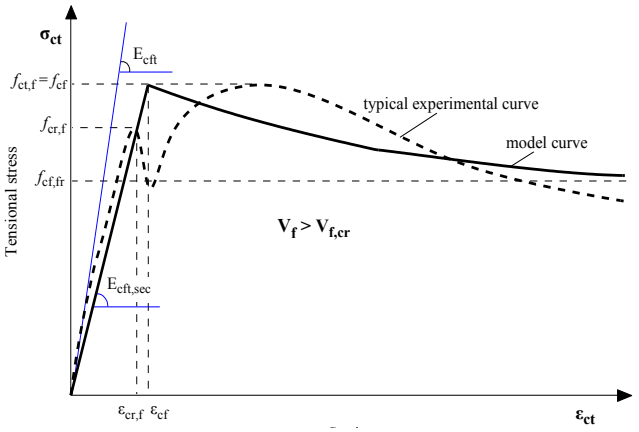

(b) Linear-exponential model

Fig. 6 Simulated stress-strain curves for the direct tensional response of SFC

$$f_{cf}=n_\ell n_o \sigma_{fu} V_f \quad (23)$$

$$\varepsilon_{cf}=a_f \varepsilon_{cr,f} \quad (24)$$

$$a_f=\begin{Bmatrix} 2 & \text{straigh fibres} \\ 3\div 8 & \text{short hooked fibres} \end{Bmatrix} \quad (25)$$

- Linear-exponential model: $V_f > V_{f,cr}$ and $f_{cf} > f_{cr,f}$: The ultimate tensile strength of SFC, $f_{ct,f}$, the corresponding strain, ε_{cf}, the value of the characteristic stress, $f_{cf,fr}$ (the descending exponential curve asymptotically tends to this stress) and the post-cracking exponential curve are calculated by the following expressions (Bentur and Mindess 2007, Karayannis 1995)

$$f_{ct,f}=f_{cr,f}=\varepsilon_{cr,f}E_{cft,\sec} \quad (26)$$

$$f_{cf}=n_\ell n_o \sigma_{fu} V_f \quad (27)$$

$$\varepsilon_{cf}=a_f \varepsilon_{cr,f} \quad (28)$$

$$\tau_{fr}=\frac{P_{fr}}{\pi d_f \ell_{fr}} \quad (29)$$

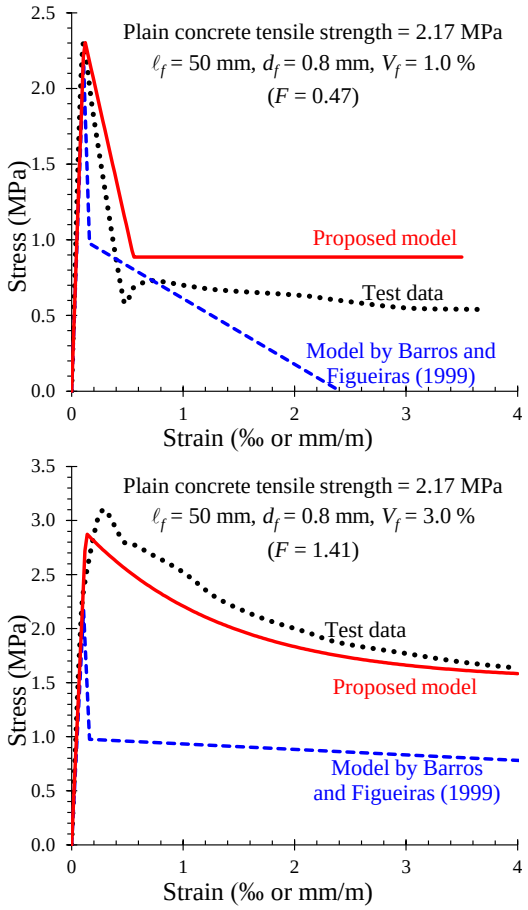

Fig. 7(a) Comparisons of the compressive stress-strain curves using tests of Karayannis (2000a)

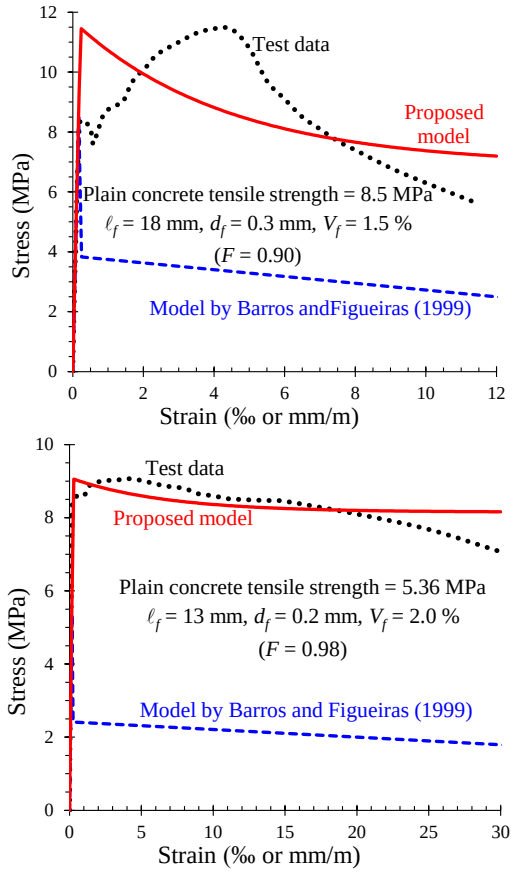

Fig. 7(b) Comparisons of the compressive stress-strain curves using tests of Wille *et al.* (2014) for V_f=1.5% and Hassan *et al.* (2012) for V_f=2%

$$\sigma_{ct} = f_{cf,fr} + \left(f_{ct,f} - f_{cf,fr}\right) e^{-k\left(\frac{\varepsilon_{ct}}{\varepsilon_{cf}} - 1\right)} \quad \text{when } \varepsilon_{ct} > \varepsilon_{cf} \quad (k = 0.1 \div 0.7) \tag{30}$$

Based on the above expressions the formulation of the entire tensional stress-strain curves for each case of SFC is as follows

For $V_f \le V_{f,cr}$:

$$\sigma_{ct} = \begin{cases} \dfrac{f_{ct,f}}{\varepsilon_{cr,f}} \varepsilon_{ct} & \text{if } 0 < \varepsilon_{ct} \le \varepsilon_{cr,f} \\ f_{ct,f} - \dfrac{f_{ct,f} - f_{cf}}{\varepsilon_{cf} - \varepsilon_{cr,f}} \left(\varepsilon_{ct} - \varepsilon_{cr,f}\right) & \text{if } \varepsilon_{cr,f} < \varepsilon_{ct} \le \varepsilon_{cf} \\ f_{cf} & \text{if } \varepsilon_{cf} < \varepsilon_{ct} \end{cases} \tag{31}$$

For $V_f > V_{f,cr}$:

$$\sigma_{ct} = \begin{cases} \dfrac{f_{cf}}{\varepsilon_{cf}} \varepsilon_{ct} & \text{if } 0 < \varepsilon_{ct} \le \varepsilon_{cf} \\ f_{cf,fr} + \left(f_{ct,f} - f_{cf,fr}\right) e^{-k\left(\frac{\varepsilon_{ct}}{\varepsilon_{cf}} - 1\right)} & \text{if } \varepsilon_{cf} < \varepsilon_{ct} \end{cases} \tag{32}$$

In order to estimate the feasibility of the proposed model to accurately describe the entire tensile response of various SFC mixtures with different amount and types of fibres Figs. 7(a), (b) and (c) have been illustrated. In these Figs. analytical tensile stress-strain curves derived from the proposed approach (red continuous lines) and the model reported in Barros and Figueiras (1999) (blue dashed lines) are compared with uniaxial tension tests (black dotted lines) of:

- Karayannis (2000a) for V_f =1% and 3% (Fig. 7(a)),
- Wille *et al.* (2014) for V_f =1.5% and Hassan *et al.* (2012) for V_f =2% (Fig. 7(b)), and
- Li *et al.* (1998) for V_f =2% and 3% and for two different types of steel fibres (Fig. 7(c)).

These comparisons imply that the proposed approach yields realistic stress-strain curves for the entire response of SFC under tension.

4. Flexural model

Most of the existing analytical models for the evaluation of the flexural capacity of concrete members reinforced with longitudinal bars and steel fibres take into account the contribution of the fibres only in the tensional zone. The extra tensile strength component due to the presence of steel fibres is added to the strength of the reinforcing bars in

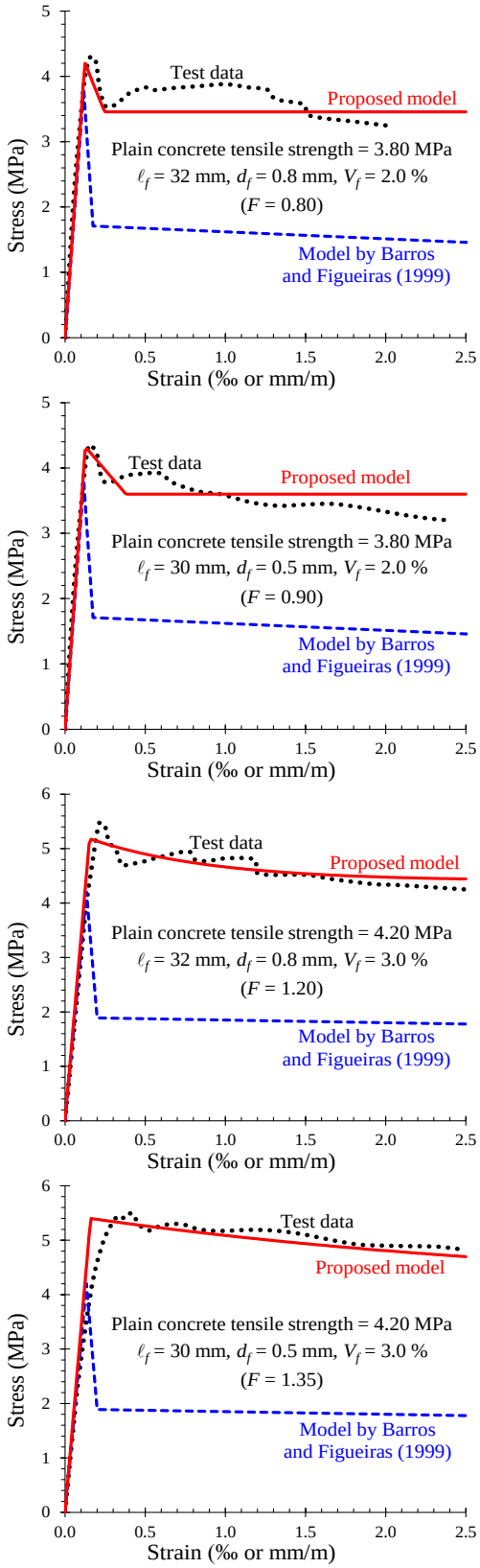

Fig. 7(c) Comparisons of the compressive stress-strain curves using tests of Li *et al*. (1998)

tension. This methodology is also adopted by Code provisions, guidelines and reports (CNR 2007, RILEM TC 162-TDF 2003, TR63 2007) for the design of SFC members

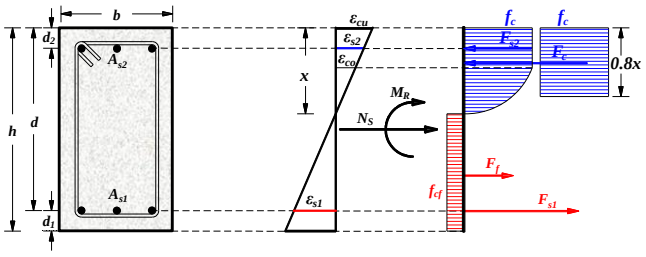

Fig. 8 Simplified flexural sectional analysis (CNR 2007, RILEM TC 162-TDF 2003, TR63 2007)

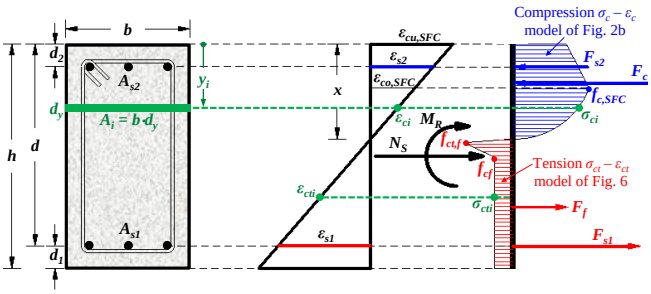

Fig. 9 Proposed SFC analysis - Sectional segmentation - Typical strain and stress distribution

under bending. The compressive stress-strain relationship of EC2 (CEN 2004) for plain concrete is adopted assuming that the influence of the fibres to the ultimate compressive stress and to the corresponding strain is negligible. For the case of tension, a simplified assumption is considered; a uniform tensile strength component along the total depth of the tensional zone due to the presence of steel fibres is simply added to the tensional force of the longitudinal steel reinforcing bars (Fig. 8).

In this study, a new numerical model is developed for the analysis of SFC structural members under bending moment and axial force. The entire moment-curvature relationship can be calculated by sectional analysis of SFC using non-linear laws for the materials that include softening response under compression and tension. The analytical solution is based on the segmentation of a SFC section to a given number of finite sectional elements that form a horizontal mesh along the total depth, h, of the cross-section (Fig. 9). The stress shape function of each segment is assumed to be constant in its depth, d_y, and obviously, lower values of this depth, or else higher number of segments, increase the accuracy of the results.

The use of refined and verified stress-strain constitutive laws for the SFC in compression and in tension that include post-peak softening parts (see Figs. 2(b) and 6, respectively), along with the ability of easy software implementation are the main innovations of the proposed numerical model with regards to the existing ones. Simple elasto-plastic curves or detailed stress-strain relationships with strain hardening for the optional conventional steel reinforcement could also be employed. The proposed model can be applied in SFC members with arbitrary cross-sectional geometry, with or without longitudinal reinforcing bars.

Assumptions of the proposed model are more or less the

Table 1 Geometrical, mechanical and reinforcement properties of the tested beams derived from the literature and analytical results of the proposed model concerning the properties of the SFC

	Specimen code name	Dimensions and plain concrete				Steel bars			Short steel fibres				SFC properties (model)			
		b (mm)	h (mm)	d_1 (mm)	f_c (MPa)	ρ_1 (%)	$f_{y\ell}$ (MPa)	$f_{u\ell}$ (MPa)	V_f (%)	ℓ_f/d_f	F	f_{uf} (MPa)	$\varepsilon_{cu,SFC}$ (‰)	$f_{c,SFC}$ (MPa)	f_{cf} (MPa)	$f_{ct,f}$ (MPa)
1	S-4-0.0	170	300	35	86.1	1.39	630	788	0.00	0	0.00	1100	3.50	86.1	0.00	4.91
	S-4-0.5	170	300	35	86.1	1.39	630	788	0.50	75	0.28	1100	3.53	91.5	0.76	5.04
	S-4-1.0	170	300	35	86.1	1.39	630	788	1.00	75	0.56	1100	5.49	96.9	1.52	5.18
	S-4-1.5	170	300	35	86.1	1.39	630	788	1.50	75	0.84	1100	7.86	102.3	2.28	5.32
	S-6-0.0	170	300	35	86.1	1.39	630	788	0.00	0	0.00	1100	3.50	86.1	0.00	4.91
	S-6-0.5	170	300	35	86.1	1.39	630	788	0.50	75	0.28	1100	3.53	91.5	0.76	5.04
	S-6-1.0	170	300	35	86.1	1.39	630	788	1.00	75	0.56	1100	5.49	96.9	1.52	5.18
	S-6-1.5	170	300	35	86.1	1.39	630	788	1.50	75	0.84	1100	7.86	102.3	2.28	5.32
2	S2-0	500	75	4	65.8	0.11	560	800	0.00	0	0.00	1100	3.50	65.8	0.00	4.90
	S2-30	500	75	4	65.8	0.11	560	800	0.38	75	0.29	1100	3.56	70.0	0.58	5.00
	S2-45	500	75	4	65.8	0.11	560	800	0.57	75	0.43	1100	4.50	72.1	0.87	5.05
	S2-60	500	75	4	65.8	0.11	560	800	0.76	75	0.57	1100	5.54	74.1	1.16	5.11
3	M80	150	300	30	33.6	1.14	560	670	1.03	55	0.42	1200	4.48	36.9	1.15	3.31
	M100	150	300	30	33.6	1.14	560	670	1.28	55	0.53	1200	5.22	37.7	1.42	3.35
	M200	150	300	30	33.6	1.14	560	670	2.56	55	1.06	1200	9.93	41.8	2.87	3.60
4	B-0.0-N2	200	250	35	48.6	1.18	530	635	0.00	0	0.00	1100	3.50	48.6	0.00	3.69
	B-0.5-N2	200	250	35	48.6	1.18	530	635	0.50	75	0.28	1100	3.53	51.8	0.76	3.81
	B-1.0-N2	200	250	35	48.6	1.18	530	635	1.00	75	0.56	1100	5.49	54.9	1.52	3.92
	B-0.0-N3	200	250	35	48.6	1.77	530	635	0.00	0	0.00	1100	3.50	48.6	0.00	3.69
	B-0.5-N3	200	250	35	48.6	1.77	530	635	0.50	75	0.28	1100	3.53	51.8	0.76	3.81
	B-1.0-N3	200	250	35	48.6	1.77	530	635	1.00	75	0.56	1100	5.49	54.9	1.52	3.92
	B-0.0-N4	200	250	35	48.6	2.37	530	635	0.00	0	0.00	1100	3.50	48.6	0.00	3.69
	B-0.5-N4	200	250	35	48.6	2.37	530	635	0.50	75	0.28	1100	3.53	51.8	0.76	3.81
	B-1.0-N4	200	250	35	48.6	2.37	530	635	1.00	75	0.56	1100	5.49	54.9	1.52	3.92
	B-0.0-M2	200	250	35	78.5	1.18	530	635	0.00	0	0.00	1100	3.50	78.5	0.00	5.05
	B-0.5-M2	200	250	35	78.5	1.18	530	635	0.50	75	0.28	1100	3.53	83.4	0.76	5.19
	B-1.0-M2	200	250	35	78.5	1.18	530	635	1.00	75	0.56	1100	5.49	88.3	1.52	5.32
	B-0.0-M3	200	250	35	78.5	1.77	530	635	0.00	0	0.00	1100	3.50	78.5	0.00	5.05
	B-0.5-M3	200	250	35	78.5	1.77	530	635	0.50	75	0.28	1100	3.53	83.4	0.76	5.19
	B-1.0-M3	200	250	35	78.5	1.77	530	635	1.00	75	0.56	1100	5.49	88.3	1.52	5.32
	B-0.0-M4	200	250	35	78.5	2.37	530	635	0.00	0	0.00	1100	3.50	78.5	0.00	5.05
	B-0.5-M4	200	250	35	78.5	2.37	530	635	0.50	75	0.28	1100	3.53	83.4	0.76	5.19
	B-1.0-M4	200	250	35	78.5	2.37	530	635	1.00	75	0.56	1100	5.49	88.3	1.52	5.32
	B-0.0-H2	200	250	35	102.4	1.18	530	635	0.00	0	0.00	1100	3.50	102.4	0.00	5.59
	B-0.5-H2	200	250	35	102.4	1.18	530	635	0.50	75	0.28	1100	3.53	108.8	0.76	5.73
	B-1.0-H2	200	250	35	102.4	1.18	530	635	1.00	75	0.56	1100	5.49	115.2	1.52	5.88
	B-0.0-H3	200	250	35	102.4	1.77	530	635	0.00	0	0.00	1100	3.50	102.4	0.00	5.59
	B-0.5-H3	200	250	35	102.4	1.77	530	635	0.50	75	0.28	1100	3.53	108.8	0.76	5.73
	B-1.0-H3	200	250	35	102.4	1.77	530	635	1.00	75	0.56	1100	5.49	115.2	1.52	5.88
	B-0.0-H4	200	250	35	102.4	2.37	530	635	0.00	0	0.00	1100	3.50	102.4	0.00	5.59
	B-0.5-H4	200	250	35	102.4	2.37	530	635	0.50	75	0.28	1100	3.53	108.8	0.76	5.73
	B-1.0-H4	200	250	35	102.4	2.37	530	635	1.00	75	0.56	1100	5.49	115.2	1.52	5.88

1: Ashour and Wafa (1993)
2: Barros and Figueiras (1999)
3: Zeris *et al.* (2009)
4: Ashour *et al.* (2000)

same as the commonly used sectional analyses:

• Sections perpendicular to the longitudinal axis before loading remain plane and perpendicular to the axis after bending.

• Perfect bond between the reinforcement and the concrete exists and therefore reinforcement strain equals to the concrete strain at the same level.

• The strains of both concrete and reinforcement are directly proportional to the distance from the neutral axis.

• The adopted constitutive laws for SFC in compression

and in tension are illustrated in Figs. 2(b) and 5, respectively, and determined in the stress-strain relationships (8) and (31) or (32), respectively.

Fig. 9 demonstrates the sectional segmentation, the strain and stress distribution along the depth, the internal forces of the materials, the externally applied axial load and the resisting bending moment based on the proposed model. The illustrated cross-section represents a typical SFC member with compressive and tensional steel bars. Further, the well-known equations for the derivation of bending moment versus curvature curves are used (see also Fig. 9).

Based on the notation of Fig. 9, the stresses of each SFC sectional segment under compression, σ_{ci}, or tension, σ_{cti}, are computed based on the corresponding strains, ε_{ci}, or ε_{cti}, respectively, using the stress-strain relationships of Eq. (8) or Eqs. (31), (32), respectively, and presented in Fig. 2(b) or Fig. 6, respectively, where i=1 to n_s, where n_s is the number of segments along the total depth, h, of the cross-section with constant depth, d_y. The stresses of the conventional steel reinforcement at each layer, σ_{sj}, are also estimated based on the corresponding strains, ε_{sj}, and the adopted stress-strain relationship (j=1 to n_r, where n_r is the number of layers of the steel reinforcing bars that is usually equal to 1 or 2 for singly or doubly reinforced members, respectively).

It is also noted that, as shown in Fig. 9, x is the depth of the compression zone, $\varepsilon_{cu,SFC}$ is the ultimate strain in the compression zone, ε_{s1} is the strain of the first steel reinforcement layer from the bottom surface of the cross-section, d_j is the distance from the upper surface of the cross-section to the centre of each longitudinal steel reinforcement layer, d is the effective depth of the cross-section, y_i is the distance from the upper surface of the cross-section to the centre of each sectional segment, A_i is the cross section area of each sectional segment, b is the width of the cross-section, F_{ci} is the SFC compressive force of each sectional segment, F_{fi} is the SFC tensile force of each sectional segment, F_{sj} is the force of each longitudinal steel reinforcement layer and A_{sj} is the area of each longitudinal steel reinforcement layer.

5. Applications and verification with test data

The developed numerical approach has been applied to 42 SFC beams subjected to predominant flexural loading in order to establish the validity of the proposed model based on a broad range of parametric studies. The database of experimental information was compiled from 4 existing works of the literature (Ashour and Wafa 1993, Barros and Figueiras 1999, Zeris *et al.* 2009, Ashour *et al.* 2000). All these tests are beams with longitudinal reinforcing bars and adequate amount of steel transverse reinforcement (stirrups) that failed due to flexure. The reference non-fibrous concrete beams used as control specimens in each work were also considered in the database.

The SFC beams included in the database contain various types of short steel fibres in different volume fractions. Table 1 presents the geometrical, the mechanical and the reinforcement data of the SFC beams of the literature and the main analytical results of the proposed numerical model concerning the properties of the SFC. These calculated results are:

- The ultimate strain in the compression zone, $\varepsilon_{cu,SFC}$,
- the compressive strength, $f_{c,SFC}$,
- the ultimate post-cracking tensile stress, f_{cf}, and
- the ultimate tensile strength, $f_{ct,f}$.

From the comparison of the material properties presented in Table 1 it is concluded that SFC has increased strength and especially strain in compression with regards to the corresponding plain concrete. The ultimate strain of SFC in the compression zone is higher than the maximum considered value for plain concrete (3.5‰) even for low volume fractions of the added steel fibres. This is an important factor that significantly influences the sectional analysis of the flexural SFC members. Further, the values of the ultimate post-cracking tensile stress and the ultimate tensile strength of SFC reveal that in most of the examined cases the tri-linear model is adopted since the volume fraction of the added steel fibres, V_f, is less than the critical one, $V_{f,cr}$, and therefore: $f_{ct,f}=f_{cr,f}>f_{cf}$.

Further, Table 2 summarizes and compare the analytical results derived from the proposed approach and the corresponding experimental data concerning the values of the resisting bending moment at yield and at ultimate. Especially, the following values are presented:

(a) Analytical values from the sectional analysis of the proposed method:

- The depth of the compression zone at yield, x_y, and at ultimate, x_u,
- the tensile force of the SFC at yield, F_{fy}, and at ultimate, F_{fu},
- the curvature at yield, φ_y, and at ultimate, φ_u,
- the ultimate strain at failure in the compression zone, ε_c, which is in the most of the examined cases equal to the value of $\varepsilon_{u,SFC}$ with the exception of the tested beams by Barros and Figueiras (1999) where the final failure was due to the fracture of the tensile steel reinforcing bars,
- the strain of the first steel reinforcement layer from the bottom surface of the cross-section, ε_{s1}, and
- the resisting bending moment at yield, $M_{y,prop}$, and at ultimate, $M_{u,prop}$.

(b) Calculated values from the flexural model developed in Barros and Figueiras (1999):

- The resisting bending moment at yield, $M_{y,calc}$, and at ultimate, $M_{u,calc}$.

(c) Test data and comparisons with analytical results:

- The experimentally observed bending moment at yield, $M_{y,exp}$, and at ultimate, $M_{u,exp}$,
- the ratios of the experimental to the analytical bending moment derived from the proposed method $M_{y,exp}/M_{y,prop}$ and $M_{u,exp}/M_{u,prop}$, and the model developed in Barros and Figueiras (1999) $M_{y,exp}/M_{y,calc}$ and $M_{u,exp}/M_{u,calc}$, at yield and at ultimate, respectively.

The comparisons in Table 2 reveal that in the majority of the examined cases a very good agreement between the experimentally observed bending moment values (at yield and at ultimate) and the analytically calculated ones is achieved. Especially, the predictions of the proposed method for the examined 42 beam specimens have mean values 1.00 and 1.02 with standard deviations 0.051 and

Table 2 Results of the experimental and the analytical values of the resisting bending moment at yield and at ultimate

	Specimen code name	Proposed method: Analytical results at yield						Proposed method: Analytical results at ultimate				Analytical calculations*			Test data and comparisons (experimental/analytical)				
		x_y (mm)	F_{fy} (kN)	φ_y (km^{-1})	$M_{y,prop}$ (kNm)	ε_{s1} (‰)	ε_c (‰)	x_u (mm)	F_{fu} (kN)	φ_u (km^{-1})	$M_{u,prop}$ (kNm)	$M_{y,calc}$ (kNm)	$M_{u,calc}$ (kNm)	$M_{y,exp}$ (kNm)	$\frac{M_{y,exp}}{M_{y,prop}}$	$\frac{M_{y,exp}}{M_{y,calc}}$	$M_{u,exp}$ (kNm)	$\frac{M_{u,exp}}{M_{u,prop}}$	$\frac{M_{u,exp}}{M_{u,calc}}$
1	S-4-0.0	64	0.0	15.7	95.9	21.1	3.5	38	0.0	93.1	105.8	90.3	97.9	98.3	1.03	1.09	105.7	1.00	1.08
	S-4-0.5	72	45.8	16.3	100.7	20.1	3.5	40	31.9	89.3	109.2	90.4	99.4	101.8	1.01	1.13	116.5	1.07	1.17
	S-4-1.0	78	70.5	16.8	104.4	33.4	5.5	37	36.7	146.8	113.7	95.0	101.6	107.4	1.03	1.13	122.8	1.08	1.21
	S-4-1.5	82	94.3	17.2	108.0	49.8	7.9	36	36.4	217.6	119.5	98.3	103.7	116.2	1.08	1.18	130.4	1.09	1.26
	S-6-0.0	64	0.0	15.7	95.9	21.1	3.5	38	0.0	93.1	104.7	91.2	99.0	98.9	1.03	1.08	104.6	1.00	1.06
	S-6-0.5	72	45.8	16.3	100.7	20.1	3.5	40	31.9	89.3	109.2	91.4	100.4	106.7	1.06	1.17	115.8	1.06	1.15
	S-6-1.0	78	70.5	16.8	104.4	33.4	5.5	37	36.7	146.8	113.7	96.0	102.6	108.8	1.04	1.13	118.6	1.04	1.16
	S-6-1.5	82	94.3	17.2	108.0	49.8	7.9	36	36.4	217.6	119.5	99.4	104.8	109.3	1.01	1.10	120.8	1.01	1.15
2	S2-0	8	20.6	44.6	2.10	50.0	1.3	2	1.3	292.6	2.40	2.00	2.65	2.30	1.10	1.15	2.50	1.04	0.94
	S2-30	11	38.3	46.3	2.50	50.0	2.2	3	30.8	735.9	3.40	2.25	3.35	2.50	1.00	1.11	3.20	0.94	0.96
	S2-45	12	49.2	47.3	2.90	50.0	2.6	4	45.6	741.2	3.90	2.55	3.90	2.85	0.98	1.12	3.75	0.96	0.96
	S2-60	13	59.8	48.2	3.30	50.0	3.0	4	60.1	746.2	4.50	2.85	5.20	2.95	0.89	1.04	5.15	1.14	0.99
3	M80	106	39.4	17.1	69.5	12.2	4.5	72	40.5	61.8	73.2	62.5	65.5	70.2	1.01	1.12	74.6	1.02	1.14
	M100	109	46.0	17.4	70.6	14.3	5.2	72	49.4	72.4	74.9	63.7	65.8	71.3	1.01	1.12	80.9	1.08	1.23
	M200	119	78.3	18.6	75.7	27.1	10.0	72	97.1	137.2	84.2	65.3	66.9	78.1	1.03	1.20	83.9	1.00	1.25
4	B-0.0-N2	64	15.8	17.6	52.8	16.8	3.5	37	2.9	94.3	55.4	47.9	51.2	50.3	0.95	1.05	58.2	1.05	1.14
	B-0.5-N2	70	39.3	18.3	55.8	15.2	3.5	41	34.3	86.9	59.1	48.2	51.9	54.5	0.98	1.13	60.2	1.02	1.16
	B-1.0-N2	76	61.4	19.1	58.7	24.5	5.5	39	55.7	139.4	62.0	52.2	52.9	60.3	1.03	1.16	64.5	1.04	1.22
	B-0.0-N3	77	14.4	19.2	76.6	10.2	3.5	55	4.3	63.7	78.8	80.3	86.8	74.4	0.97	0.93	77.1	0.98	0.89
	B-0.5-N3	83	36.4	20.1	79.2	9.6	3.5	58	32.8	61.0	82.5	80.6	87.8	74.9	0.95	0.93	83.8	1.02	0.95
	B-1.0-N3	88	57.0	20.8	81.7	15.8	5.5	56	60.7	98.8	87.1	84.5	88.9	86.4	1.06	1.02	87.7	1.01	0.99
	B-0.0-N4	89	13.2	21.0	99.2	6.8	3.5	73	5.8	48.1	100.4	90.5	99.1	94.1	0.95	1.04	98.4	0.98	0.99
	B-0.5-N4	94	33.8	21.9	101.6	6.6	3.5	75	31.3	47.0	104.0	90.6	100.2	101.2	1.00	1.12	104.0	1.00	1.04
	B-1.0-N4	98	53.3	22.7	103.9	11.2	5.5	71	56.6	77.7	108.6	93.3	101.1	105.0	1.01	1.13	105.8	0.97	1.05
	B-0.0-M2	52	23.3	16.2	54.4	28.5	3.5	23	2.5	149.0	58.3	48.8	52.0	49.5	0.91	1.02	55.3	0.95	1.06
	B-0.5-M2	57	48.6	16.8	57.7	26.4	3.5	25	29.6	139.3	60.8	49.1	52.9	56.6	0.98	1.15	63.3	1.04	1.20
	B-1.0-M2	62	72.6	17.4	60.8	44.3	5.5	24	34.0	231.3	62.2	53.5	54.0	65.1	1.07	1.22	69.9	1.12	1.29
	B-0.0-M3	62	21.9	17.3	79.4	18.3	3.5	35	3.7	101.4	83.7	80.9	85.9	75.2	0.95	0.93	80.9	0.97	0.94
	B-0.5-M3	67	45.9	17.9	82.3	17.2	3.5	37	35.8	96.3	87.6	81.2	87.1	81.0	0.98	1.00	89.6	1.02	1.03
	B-1.0-M3	72	68.7	18.5	85.1	28.7	5.5	34	49.5	159.0	90.0	85.7	88.6	86.8	1.02	1.01	92.1	1.02	1.04
	B-0.0-M4	70	20.7	18.3	103.7	13.0	3.5	46	4.9	76.8	107.9	105.1	109.2	97.4	0.94	0.93	103.8	0.96	0.95
	B-0.5-M4	76	43.6	19.0	106.3	12.5	3.5	47	35.1	74.4	111.8	105.2	110.8	109.4	1.03	1.04	113.6	1.02	1.03
	B-1.0-M4	80	65.3	19.7	108.8	20.6	5.5	45	64.4	121.2	117.5	109.1	112.2	113.5	1.04	1.04	115.7	0.98	1.03
	B-0.0-H2	46	26.8	15.7	55.1	37.6	3.5	18	2.2	191.3	59.9	48.0	52.6	48.6	0.88	1.01	55.9	0.93	1.06
	B-0.5-H2	51	52.9	16.2	58.5	35.8	3.5	19	22.8	182.7	61.4	52.2	53.5	58.3	1.00	1.12	62.6	1.02	1.17
	B-1.0-H2	56	77.9	16.6	61.8	59.3	5.5	18	26.3	301.2	63.7	52.7	54.9	68.9	1.11	1.31	69.3	1.09	1.26
	B-0.0-H3	55	25.4	16.5	80.6	24.6	3.5	27	3.2	130.9	86.1	72.2	77.0	77.5	0.96	1.07	82.8	0.96	1.07
	B-0.5-H3	60	50.3	17.1	83.7	23.3	3.5	28	33.3	124.9	89.4	72.5	78.1	84.4	1.01	1.16	89.8	1.00	1.15
	B-1.0-H3	64	74.2	17.6	86.7	39.4	5.5	26	37.9	208.6	91.4	76.6	79.6	91.3	1.05	1.19	95.6	1.05	1.20
	B-0.0-H4	62	24.1	17.3	105.6	17.9	3.5	35	4.2	99.4	111.4	98.0	102.5	100.9	0.96	1.03	108.1	0.97	1.05
	B-0.5-H4	67	48.2	18.0	108.3	17.1	3.5	37	36.2	96.0	115.4	98.2	104.0	107.8	1.00	1.10	115.0	1.00	1.11
	B-1.0-H4	72	71.1	18.5	111.0	28.8	5.5	34	49.5	159.6	118.6	102.1	105.5	113.4	1.02	1.11	120.6	1.02	1.14
	Mean value (from 42 beam specimens):														1.00	1.09		1.02	1.09
	Standard deviation (from 42 beam specimens):														5.1%	8.3%		4.8%	10.5%

1: Ashour and Wafa (1993)
2: Barros and Figueiras (1999)
3: Zeris *et al.* (2009)
4: Ashour *et al.* (2000)

* Model developed in Barros and Figueiras (1999)

0.048 for the bending moment at yield and at ultimate, respectively. Similarly, the predictions of the model developed in Barros and Figueiras (1999) have mean values 1.09 and 1.09 with standard deviations 0.083 and 0.105 for the bending moment at yield and at ultimate, respectively.

Further, in order to verify the ability of the developed

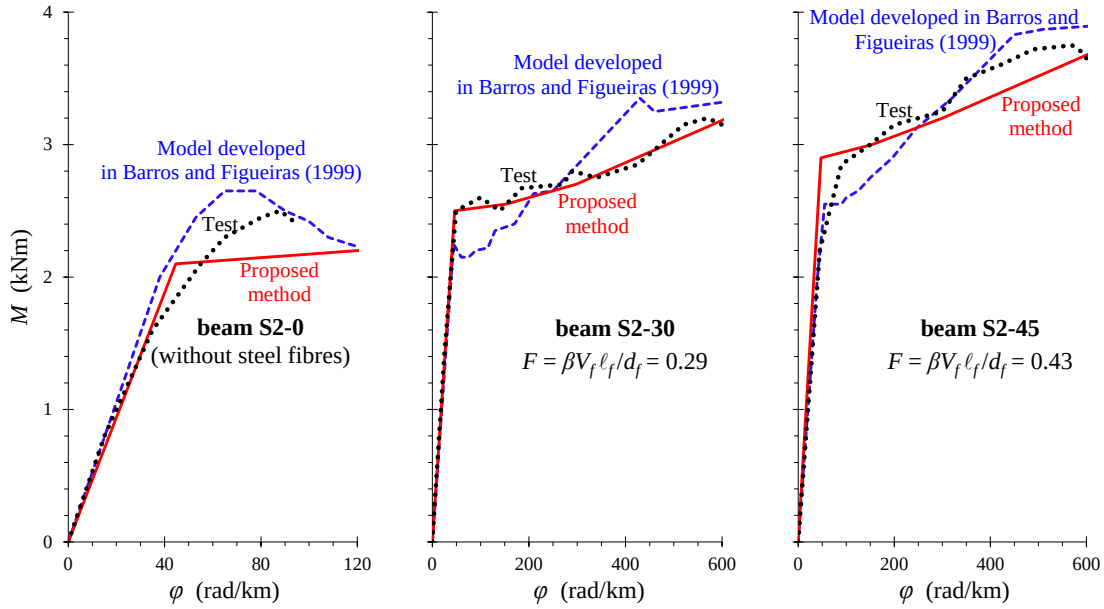

Fig. 10 Comparisons between the experimental and the analytical bending moment versus curvature curves - Tests from the study of Barros and Figueiras (1999)

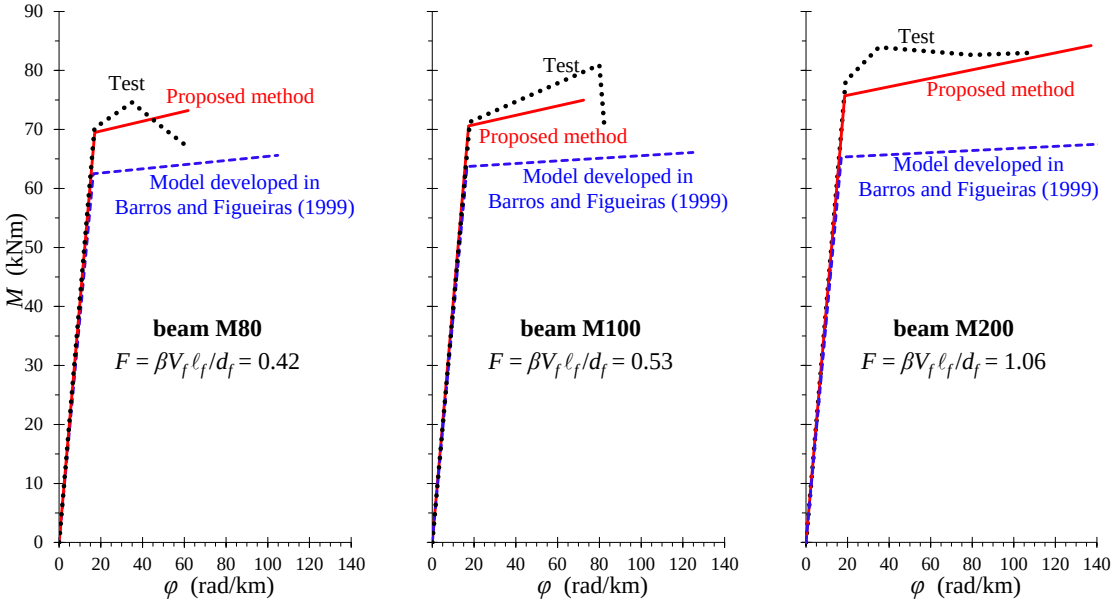

Fig. 11 Comparisons between the experimental and the analytical bending moment versus curvature curves - Tests from the study of Zeris *et al.* (2009)

numerical model to accurately predict the entire flexural behaviour of a SFC member in terms of bending moment, M, versus curvature, φ, curves, Figs. 10 and 11 compare the analytical and the experimental M–φ curves from the tests carried out by Barros and Figueiras (1999), Zeris *et al.* (2009), respectively. For comparison reasons the analytical predicted curves derived from the proposed method and the model developed in Barros and Figueiras (1999) are presented in these Figs. From these comparisons it is indicated that in most of the examined cases the analytical M–φ curves fit reasonably well to the experimentally obtained ones and therefore the proposed sectional analysis can successfully describe the overall flexural performance of a SFC structural member.

Furthermore, the differences between the results derived from the simplified flexural sectional analysis shown in Fig. 8 and the predictions of the proposed sectional analysis (see also Fig. 9) are examined in Fig. 12. The bending moment versus curvature analytical curves derived from the proposed and the simplified sectional analysis are demonstrated in Figs. 12(a) and (b), respectively. Fig. 12(c) compares the curvature ductility, μ_φ, versus the fibre factor, F, of both examined analyses that concern a rectangular cross-section shown in Fig. 12(d). It is known that the curvature ductility equals to the ratio of the curvature at ultimate to the curvature at yield.

The comparison of these analytical curves clarifies that the main difference between the predictions of the proposed

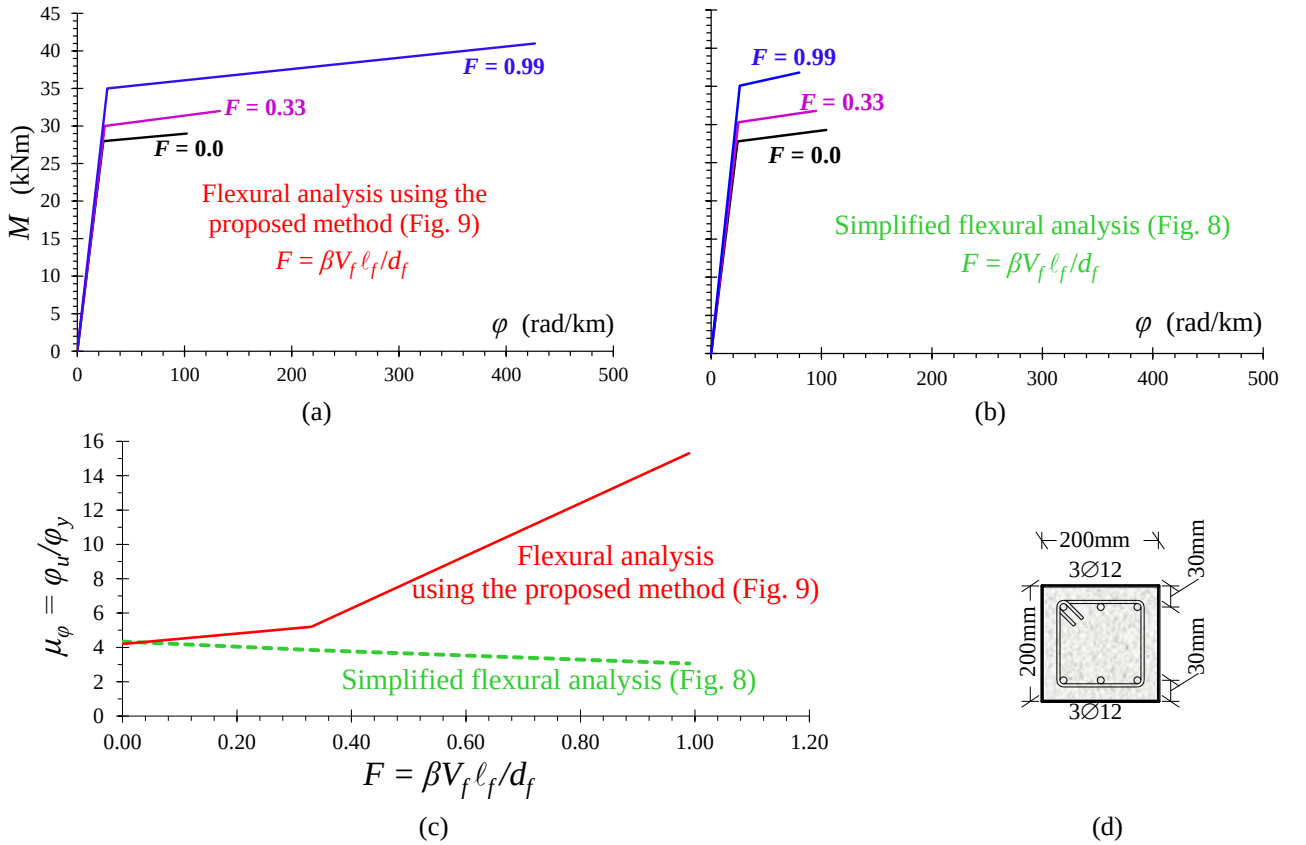

Fig. 12 Differences between the results derived from the proposed method and the simplified flexural sectional analysis

analysis and the simplified one are focused on the post-peak response and especially the predictions of the bending moment and the curvature at ultimate. The predicted values of the resisting bending moments at yield are more or less the same in both models since the influence of the steel fibres till the point of steel yielding is rather limited in the compressive zone. However, the predictions of the proposed approach provide rational and more accurate results concerning the resisting bending moment and the curvature at ultimate, and the curvature ductility, especially in the case of SFC members with higher steel fibre factor.

6. Conclusions

A numerical model for the prediction of the flexural response of fibrous concrete cross-sections in terms of bending moment versus curvature curves has been proposed in this study.

- The addition of steel fibres in concrete significantly increases the maximum compressive strain and improves the post-cracking tensile response. These favourable characteristics are meticulously considered in the developed sectional analysis which employs refined and verified stress-strain constitutive laws for the Steel Fibrous Concrete (SFC) in compression and in tension that include post-peak softening parts. Equations with feasible software implementation have been derived.
- SFC structural members with increased values of the fibre factor, *F*, exhibit enhanced flexural performance and increased ductility. The developed sectional analysis predicts accurately the overall experimental flexural behaviour and particularly the increased curvature ductility of fibrous concrete members with higher amount of steel fibres.
- The validity of the proposed model is checked through extensive comparisons between analytical predictions and test data of 42 SFC beam specimens. From these comparisons, it is observed that the developed approach predicts accurately the flexural capacity and ductility, and yields well-fitted bending moment versus curvature analytical curves to the corresponding test data. Further, it provides rational and more accurate results concerning the compressive and the tensile response of SFC mixtures, and the curvature ductility, the resisting bending moment and the curvature at ultimate of SFC cross-sections with regards to the predictions of existing models.

References

Abbas, A.A., Mohsin, S.M.S. and Cotsovos, D.M. (2014), "Seismic response of steel fibre reinforced concrete beam-column joints", *Eng. Struct.*, **67**, 261-283.

Amato, G., Campione, G., Cavaleri, L. and Minafó, G. (2011), "Flexural behaviour of external R/C steel fibre reinforced beam-column joints", *Eur. Environ. Civil Eng.*, **15**(9), 1253-1276.

Ashour, S.A. and Wafa, F.F. (1993), "Flexural behavior of high-strength fiber reinforced concrete beams", *ACI Struct.*, **90**(3), 279-287.

Ashour, S.A., Wafa, F.F. and Kamal, M.I. (2000), "Effect of the concrete compressive strength and tensile reinforcement ratio on the flexural behavior of fibrous concrete beams", *Eng. Struct.*, **22**(9), 1145-1158.

Aslani, F. and Natoori, M. (2013), "Stress-strain relationships for steel fibre reinforced self-compacting concrete", *Struct. Eng. Mech.*, **46**(2), 295-322.

Aslani, F. and Nejadi, S. (2012), "Bond characteristics of steel fibre reinforced self-compacting concrete", *Can. Civil Eng.*, **39**(7), 834-848.

Aslani, F., Nejadi, S. and Samali, N. (2014), "Long-term flexural cracking control of reinforced self-compacting concrete one way slabs with and without fibres", *Comput. Concrete*, **14**(4), 419-444.

Barros, J.A. and Figueiras, J.A. (1999), "Flexural behaviour of SFRC: Testing and modeling", *J. Mater. Civil Eng.*, **11**(4), 331-339.

Bentur, A. and Mindess, S. (2007), *Fibre Reinforced Cementitious Composites*, Modern Concrete Technology Series Second, Taylor & Francis, New York.

Cagatay, I. and Dincer, R. (2011), "Modeling of concrete containing steel fibers: Toughness and mechanical properties", *Comput. Concrete*, **8**(3), 357-369.

Campione, G. (2015), "Analytical prediction of load deflection curves of external steel fibers R/C beam-column joints under monotonic loading", *Eng. Struct.*, **83**(11), 86-98.

Campione, G. and Mangiavillano, M.L. (2008), "Fibrous reinforced concrete beams in flexure: Experimental investigation, analytical modelling and design considerations", *Eng. Struct.*, **30**, 2970-2980.

CEN (2004), Eurocode 2. Design of Concrete Structures–Part 1–1: General Rules and Rules for Buildings (EN 1992-1-1), Brussels.

Chalioris, C.E. (2013a), "Analytical approach for the evaluation of minimum fibre factor required for steel fibrous concrete beams under combined shear and flexure", *Constr. Build. Mater.*, **43**(1), 317-336.

Chalioris, C.E. (2013b), "Steel fibrous RC Beams subjected to cyclic deformations under predominant shear", *Eng. Struct.*, **49**(1), 104-118.

Chalioris, C.E. and Karayannis, C.G. (2009), "Effectiveness of the use of steel fibres on the torsional behaviour of flanged concrete beams", *Cement Concrete Compos.*, **31**(5), 331-341.

Chalioris, C.E. and Liotoglou, F.A. (2015), "Tests and simplified behavioural model for steel fibrous concrete under compression", *Adv. Civil Eng. Build. Mater.*, **4**(1), 195-199.

Chalioris, C.E. and Sfiri, E.F. (2011), "Shear performance of steel fibrous concrete beams", *Proc. Eng.*, **14**(1), 2064-2068.

CNR (2007), Guide for the Design and Construction of Fiber-Reinforced Concrete Structures (CNR-DT 204/2006), Rome.

Colajanni, P., Recupero, A. and Spinella, N. (2012), "Generalization of shear truss model to the case of SFRC beams with stirrups", *Comput. Concrete*, **9**(3), 227-244.

Cuenca, E., Echegaray-Oviedo, J. and Serna, P. (2015), "Influence of concrete matrix and type of fiber on the shear behavior of self-compacting fiber reinforced concrete beams", *Compos. Part B: Eng.*, **75**, 135-147.

Daniel, L. and Loukili, A. (2002), "Behavior of high-strength fiber-reinforced concrete beams under cyclic loading", *ACI Struct.*, **99**(3), 248-256.

Duzgun, O.A., Gul, R. and Aydin, A.C. (2005), "Effect of steel fibers on the mechanical properties of natural lightweight aggregate concrete", *Mater. Lett.*, **59**(27), 3357-3363.

Fu, Q., Ma, Q., Jin, X., Shah, A. and Tian, Y. (2014), "Fracture property of steel fiber reinforced concrete at early age", *Comput. Concrete*, **13**(1), 31-47.

Gao, J., Sun, W. and Morino, K. (1997), "Mechanical properties of steel fiber-reinforced, high-strength, lightweight, concrete", *Cement Concrete Compos.*, **19**(4), 307-313.

Greenough, T. and Nehdi, M. (2008), "Shear behavior of fiber-reinforced self-consolidating concrete slender beams", *ACI Matet.*, **105**(5), 468-477.

Hassan, A.M.T., Jones, S.W. and Mahmud, G.H. (2012), "Experimental test methods to determine the uniaxial tensile and compressive behaviour of ultra high performance fibre reinforced concrete (UHPFRC)", *Constr. Build. Mater.*, **37**, 874-882.

Jain, K. and Singh, B. (2016), "Deformed steel fibres as minimum shear reinforcement - An investigation", *Struct.*, **7**, 126-137.

Kara, F.I. and Dundar, C. (2012), "Prediction of deflection of high strength steel fiber reinforced concrete beams and columns", *Comput. Concrete*, **9**(2), 133-151.

Karayannis, C.G. (1995), "A numerical approach to steel-fibre reinforced concrete under torsion", *Struct. Eng. Rev.*, **7**(2), 83-91.

Karayannis, C.G. (2000a), "Nonlinear analysis and tests of steel-fiber concrete beams in torsion", *Struct. Eng. Mech.*, **9**(4), 323-338.

Karayannis, C.G. (2000b), "Analysis and experimental study for steel fibre pullout from cementitious matrices", *Adv. Compos. Lett.*, **9**(4), 243-255.

Köksal, F., Altun, F., Yiğit, I. and Şahin, Y. (2008), "Combined effect of silica fume and steel fiber on the mechanical properties of high strength concretes", *Constr. Build. Mater.*, **22**(8), 1874-1880.

Kotsovos, G., Zeris, C. and Kotsovos, M. (2007), "The effect of steel fibres on the earthquake-resistant design of reinforced concrete structures", *Mater. Struct.*, **40**(1), 175-188.

Kwak, Y.K., Eberhard, M.O., Kim, W.S. and Kim, J. (2002), "Shear strength of steel siber-reinforced concrete beams without stirrups", *ACI Struct.*, **99**(4), 530-538.

Li, Z., Li, F., Chang, T.Y.P. and Mai, Y.W. (1998), "Uniaxial tensile behavior of concrete reinforced with randomly distributed short fibers", *ACI Mater.*, **95**(5), 564-574.

Manolis, D., Gareis, J., Tsonos, A. and Neal, J. (1997), "Dynamic properties of polypropylene fiber-feinforced concrete slabs", *Cement Concrete Compos.*, **19**(4), 341-349.

Marar, K., Eren, O. and Yitmen, I. (2011), "Compression specific toughness of normal strength steel fiber reinforced concrete (NSSFRC) and high strength steel fiber reinforced concrete (HSSFRC)", *Mater. Res.*, **14**(2), 239-247.

Mohammadi, Y., Singh, S.P. and Kaushik, S.K. (2008), "Properties of steel fibrous concrete containing mixed fibres in fresh and hardened state", *Constr. Build. Mater.*, **22**(5), 956-965.

Naaman, A.E. (2003), "Engineered steel fibers with optimal properties for reinforcement of cement composites", *Adv. Concrete Tech.*, **1**(3), 241-252.

Narayanan, R. and Darwish, I.Y.S. (1987), "Use of steel fibers as shear reinforcement", *ACI Struct.*, **84**(3), 216-227.

Nataraja, M.C., Dhang, N. and Gupta, A.P. (1999), "Stress-strain curves for steel-fiber reinforced concrete under compression", *Cement Concrete Compos.*, **21**(5-6), 383-390.

Nehdi, M., Abbas, S. and Soliman, A. (2015), "Exploratory study of ultra-high performance fiber reinforced concrete tunnel lining segments with varying steel fiber lengths and dosages", *Eng. Struct.*, **101**(1), 733-742.

Nili, M. and Afroughsabet, V. (2012), "Property assessment of steel-fibre reinforced concrete made with silica fume", *Constr. Build. Mater.*, **28**, 664-669.

Oliveira Júnior, L.A., Borges, V.E.S, Danin, A.R., Machado, D.V.R., Araujo, D.L., Debs M.K.E. and Rodrigues, P.F. (2010), "Stress-strain curves for steel fiber-reinforced concrete in compression", *Rev. Mater.*, **15**(2), 60-266.

Padmarajaiah, S.K. and Ramaswamy, A. (2001), "Behavior of

fiber-reinforced prestressed and reinforced high-strength concrete beams subjected to shear", *ACI Struct.*, **98**(5), 752-761.
Pawade, P.Y., Nagarnaik, P.B. and Pande, A.M. (2011), "Performance of steel fiber on standard strength concrete in compression", *Civil Struct. Eng.*, **2**(2), 483-492.
RILEM TC 162-TDF (2003), "Test and design methods for steel fibre reinforced concrete, σ-ε design method. Final recommendation", *Mater. Struct.*, **36**(262), 560-567.
Singh, H. (2015), "Flexural modeling of steel fiber-reinforced concrete members: Analytical investigations", *Pract. Period. Struct. Des. Constr.*, **20**(4), 04014046.
Singh, H. (2016), "Flexural modelling of steel-fibre-reinforced concrete member with conventional tensile rebars", *Proc. Inst. Civil Eng.: Struct. Build.*, **169**(1), 54-66.
Song, P.S. and Hwang, S. (2004), "Mechanical properties of high-strength steel fiber-reinforced concrete", *Constr. Build. Mater.*, **18**(9), 669-673.
Soulioti, D.V., Barkoula, N.M., Paipetis, A. and Matikas, T.E. (2011), "Effects of fibre geometry and volume fraction on the flexural behaviour of steel-fibre reinforced concrete", *Strain*, **47**(1), 535-541.
Spinella, N. (2013), "Shear strength of full-scale steel fibre-reinforced concrete beams without stirrups", *Comput. Concrete*, **11**(5), 365-382.
Spinella, N., Colajanni, P. and La Mendola, L. (2012), "Nonlinear analysis of beams reinforced in shear with stirrups and steel fibers", *ACI Struct.*, **109**(1), 53-64.
Spinella, N., Colajanni, P. and Recupero, A. (2010), "A simple plastic model for shear critical SFRC beams", *Struct. Eng.*, ASCE, **136**(4), 390-400.
Tan, K.H., Murugappan, K. and Paramasivam, P. (1993), "Shear behavior of steel fiber Reinforced concrete beams", *ACI Struct.*, **90**(1), 3-11.
TR63 (2007), Guidance for the Design of Steel-Fibre-Reinforced Concrete, Concrete Society, Camberley, UK.
Tsonos, A.D.G. (2009a), "Steel fiber high-strength reinforced concrete: A new solution for earthquake strengthening of old R/C structures", *WIT Tran. Build. Environ.*, **104**(1), 153-164.
Tsonos, A.D.G. (2009b), "Ultra-high-performance fiber reinforced concrete: an innovative solution for strengthening old R/C structures and for improving the FRP strengthening method", *WIT Tran. Eng. Sci.*, **64**, 273-284.
Unal, O., Demir, F. and Uygunoglu, T. (2007), "Fuzzy logic approach to predict stress-strain curves of steel fiber-reinforced concretes in compression", *Build. Environ.*, **42**(10), 3589-3595.
Wang, Z.L., Wu, J. and Wang, J.G. (2010), "Experimental and numerical analysis on effect of fiber aspect ratio on mechanical properties of SFRC", *Constr. Build. Mater.*, **24**(4), 559-565.
Wille, K., El-Tawil, S. and Naaman, A.E. (2014), "Properties of strain hardening ultra high performance fiber reinforced concrete (UHP-FRC) under direct tensile loading", *Cement Concrete Compos.*, **48**, 53-66.
Yazici, S., Inan, G. and Tabak, V. (2007), "Effect of aspect ratio and volume fraction of steel fiber on the mechanical properties of SFRC", *Constr. Build. Mater.*, **21**(6), 1250-1253.
Zeris, C., Vitalis, A. and Kontoyannis, P. (2009), "Experimental investigation of steel fiber reinforced concrete beams without shear reinforcement", *Proceedings of the 16th Hellenic Concrete Conference*, Pafos, Cyprus.

CC